Kinetic dissipation and anisotropic heating in a turbulent collisionless plasma

T. N. Parashar, M. A. Shay, P. A. Cassak,[a] and W. H. Matthaeus
Department of Physics and Astronomy, 217 Sharp Laboratory, University of Delaware, Newark, Delaware 19716, USA

(Received 14 October 2008; accepted 12 February 2009; published online 30 March 2009)

The kinetic evolution of the Orszag–Tang vortex is studied using collisionless hybrid simulations. In magnetohydrodynamics (MHD) this configuration leads rapidly to broadband turbulence. At large length scales, the evolution of the hybrid simulations is very similar to MHD, with magnetic power spectra displaying scaling similar to a Kolmogorov scaling of $-5/3$. At small scales, differences from MHD arise, as energy dissipates into heat almost exclusively through the magnetic field. The magnetic energy spectrum of the hybrid simulation shows a break where linear theory predicts that the Hall term in Ohm's law becomes significant, leading to dispersive kinetic Alfvén waves. A key result is that protons are heated preferentially in the plane perpendicular to the mean magnetic field, creating a proton temperature anisotropy of the type observed in the corona and solar wind.
 [DOI: 10.1063/1.3094062]

I. INTRODUCTION

The dissipation of turbulent energy in plasmas plays a critical role in understanding coronal heating and the acceleration of the solar wind,[1] turbulence in the interplanetary medium,[2] energy storage and release in the magnetosphere,[3] and in a variety of other plasma and astrophysical contexts.[4] By "dissipation," we mean the conversion of fluid scale energy irreversibly into kinetic degrees of freedom.

A key observational clue about the nature of this dissipation is the substantial heating of protons, often preferentially in the plane perpendicular to the mean magnetic field,[1,5] both in the solar wind [plasma β=(thermal speed/Alfvén speed)$^2 \sim 1$] and in the corona ($\beta \ll 1$). This heating has a variety of potential sources, including shocks and wave-particle interactions involving nonthermal distributions such as pickup ions, but the ubiquity of broadband Kolmogorov-type fluctuations suggests that kinetic absorption of fluid energy at or beyond the high wavenumber end of the inertial range plays an important role.

The particular mechanism allowing the kinetic absorption of fluid energy at high wavenumber is currently not well understood. Cyclotron damping of high frequency waves has been invoked as a way to anisotropically heat protons.[6–8] However, turbulence simulations and observations of the solar wind find evidence that most of the turbulent energy at high wavenumber resides in highly oblique waves, whose frequencies and parallel wavenumbers are too low to support significant cyclotron resonance (see, for example, Refs. 9–12). Many studies have attempted to resolve this discrepancy. Examinations of weak turbulence (low β) using quasilinear theory have found that three-wave interactions between fast and Alfvén waves can transfer energy to high frequencies, allowing cyclotron damping of protons.[13,14] Other studies have focused on new physics present at high wave numbers of the oblique cascade to generate anisotropic heating. Matthaeus *et al.*[15] examined turbulent reconnection sites in magnetohydrodynamics (MHD) simulations and postulated that in a real system electron phase-space holes could kinetically couple to protons, heating them. Test particles stepped through the MHD simulation fields found anisotropic heating of protons due to the nonuniform electric fields.[16] Landau damping of these oblique high wavenumber fluctuations have been postulated to create electron parallel beams, then electron phase-space holes, which would heat protons via stochastic interactions.[17] Markovskii *et al.*[18] studied a velocity shear instability that generates waves near harmonics of the ion cyclotron frequency, allowing anisotropic heating.

A fundamental self-consistent demonstration of turbulent anisotropic proton heating is needed, however, as a first step toward a basic physics understanding of the dissipation processes that heat the solar corona and solar wind. MHD is a very useful plasma model that generally employs small but nonzero viscosity and/or resistivity, but this is not easily justified for collisionless systems where the mean free path is comparable to the system size (as in most of the corona and solar wind). More sophisticated attempts to numerically model plasma dissipation, e.g., by employing hyperresistivity, hyperviscosity, or indirectly by including the Hall[15,19,20] or finite Larmor radius effects (see Ref. 21), include only selected approximations to kinetic effects and, therefore, do not include the wider range of mechanisms available to the kinetic plasma.

Kinetic simulations with variations in one dimension have been used extensively to examine particular dissipation mechanisms which may be active in turbulence (see Refs. 22 and 23 and references therein). However, one-dimensional models cannot capture nonlinear cascade processes akin to Kolmogorov-type hydrodynamic turbulence and are thus incomplete. Recently, kinetic particle in cell (PIC) simulations of a sheet pinch have been used to study mode conversion

[a]Present address: Department of Physics, Hodges Hall, Box 6315, West Virginia University, Morgantown, West Virginia 26506.

and dissipation,[24] gyrokinetic simulations have shown spectra consistent with dispersive waves,[25] and kinetic PIC simulations of whistler turbulence found a cascade of magnetic fluctuation energy and preferential heating of electrons parallel to the mean magnetic field.[26]

In this paper, we report a demonstration of turbulent anisotropic proton heating in the Orszag–Tang vortex[27] using a hybrid simulation, which includes all proton kinetic effects. The hybrid simulation results are very similar at large length scales to MHD simulations of the same system (having very similar magnetic power spectra) but show significant differences at small scales where kinetic effects are important. The magnetic power spectra of the hybrid simulations show a break at $k \approx (d_i c_s / c_m)^{-1}$, where linear two-fluid theory predicts that the Hall term becomes significant, leading to dispersive kinetic Alfvén waves (see Ref. 28 and references therein). Analysis of the hybrid results shows that energy is dissipated into proton heating almost exclusively through the magnetic field and not through the proton bulk velocity. The proton heating occurs preferentially in the plane perpendicular to the mean magnetic field. This simulation, to our knowledge, is the first self-consistent demonstration of turbulent anisotropic proton heating associated with a quasi-incompressible nonlinear MHD cascade. Finally, effective transport coefficients from the hybrid simulations are calculated, showing that the approximation of constant resistivity η is potentially reasonable (although it cannot reproduce the proton temperature anisotropy), but a constant viscosity ν is untenable.

II. HYBRID SIMULATION MODEL

The Orszag–Tang vortex[27] is a well studied MHD initial configuration given by

$$\mathbf{B} = -\sin y\hat{\mathbf{x}} + \sin 2x\hat{\mathbf{y}} + B_g\hat{\mathbf{z}}, \tag{1}$$

$$\mathbf{v} = -\sin y\hat{\mathbf{x}} + \sin x\hat{\mathbf{y}} \tag{2}$$

with $\mathbf{B}$ as the magnetic field (B_g is a uniform guide field) and $\mathbf{v}$ as the proton bulk velocity in normalized units described later. This configuration leads immediately to strong nonlinear couplings, producing cascadelike activity that might reasonably approximate the highest wavenumber decade of the inertial range. These couplings, which are dominantly local in wavenumber, in turn, drive the dissipation range. The physics of the Orszag–Tang vortex has been previously studied using incompressible[27] and compressible[29] MHD simulations. Its robust production of nonlinear activity is a motivation for its frequent use in validating numerical schemes (see, e.g., Ref. 30).

Simulating kinetic dissipation is difficult and computationally expensive due to the requirement of treating a wide range of length scales. By choosing a computational domain with approximately one decade of scale in the MHD range and another in the kinetic range, we can study the conversion of strongly driven MHD fluctuations into kinetic motions. A related earlier study of the Orszag–Tang vortex compared the global behavior of hybrid and Hall MHD simulations[31] but included a mean in-plane magnetic field while not adequately resolving the proton inertial length.

We use the hybrid code P3D in 2.5D (a parallel version of the code described in Ref. 32), which models protons as individual particles and electrons as a fluid. This code has been used extensively to simulate magnetic reconnection (see Refs. 33–36 and references therein). The code advances the following equations:

$$\frac{d\mathbf{x}_i}{dt} = \mathbf{v}_i, \tag{3}$$

$$\frac{d\mathbf{v}_i}{dt} = \frac{1}{\epsilon_H}(\mathbf{E}' + \mathbf{v}_i \times \mathbf{B}), \tag{4}$$

$$\frac{\partial \mathbf{B}'}{\partial t} = \nabla \times (\mathbf{v} \times \mathbf{B}) - \epsilon_H \nabla \times \left(\frac{\mathbf{J}}{n} \times \mathbf{B}'\right), \tag{5}$$

$$\mathbf{B}' = \left(1 - \frac{m_e}{m_i}\epsilon_H^2 \nabla^2\right)\mathbf{B}, \tag{6}$$

$$\mathbf{E}' = \mathbf{B} \times \left(\mathbf{v} - \epsilon_H \frac{\mathbf{J}}{n}\right), \tag{7}$$

where $\mathbf{J} = \nabla \times \mathbf{B}$ is the current density, $\epsilon_H \equiv c/(L_0 \omega_{pi})$ is the normalized proton inertial length, m_e and m_i are the electron and proton masses, $\mathbf{x}_i$ and $\mathbf{v}_i$ are the positions and velocities of the individual protons, and $\mathbf{v}$ is the proton bulk flow speed. Length is normalized to L_0, velocity to $V_0 = B_0/(4\pi m n_0)^{1/2}$, time to $t_0 = L_0/V_0$, and temperature to $B_0^2/(4\pi n_0)$. The average density is n_0 and B_0 is the root mean square in-plane magnetic field. The magnetic field $\mathbf{B}$ is determined from $\mathbf{B}'$ using the multigrid method. The fields are extrapolated to the particle positions using a first-order weighting scheme, which is essentially linear interpolation.[37] This allows the smooth variation due to particle motion of the fields felt by the particle. A similar first-order weighting scheme is used to determine the fluid moments at the grid locations from the particles. The code assumes quasineutrality. The electron temperature is zero and is not updated.

Hybrid simulations are ideally suited for exploring dissipation and proton heating in collisionless plasmas because they include a complete kinetic description of protons. Due to the finite temperature of the protons, kinetic Alfvén waves are present in this set of hybrid simulations (see Refs. 28 and 38 and references therein), as well as parallel proton bulk flows.

The simulation domain is a square box of side length of $2\pi \times 2\pi$ with 512×512 grid points. About 105×10^6 protons are loaded with an initial Maxwellian distribution having a uniform temperature=8, and $\epsilon_H = 2\pi/25.6$ and $m_e = 0.04 m_i$. No artificial dissipation is present other than grid scale dissipation. Choosing a guide field $B_g = 5$ (total $\beta = 2nT/B^2 \approx 0.62$) reduces the system compressibility. Incompressibility is further promoted by adding perturbations to the background density n_0 that enforce $\partial(\nabla \cdot \mathbf{v})/\partial t = 0$ at $t = 0$. Simulations without the added perturbation show only small differences.

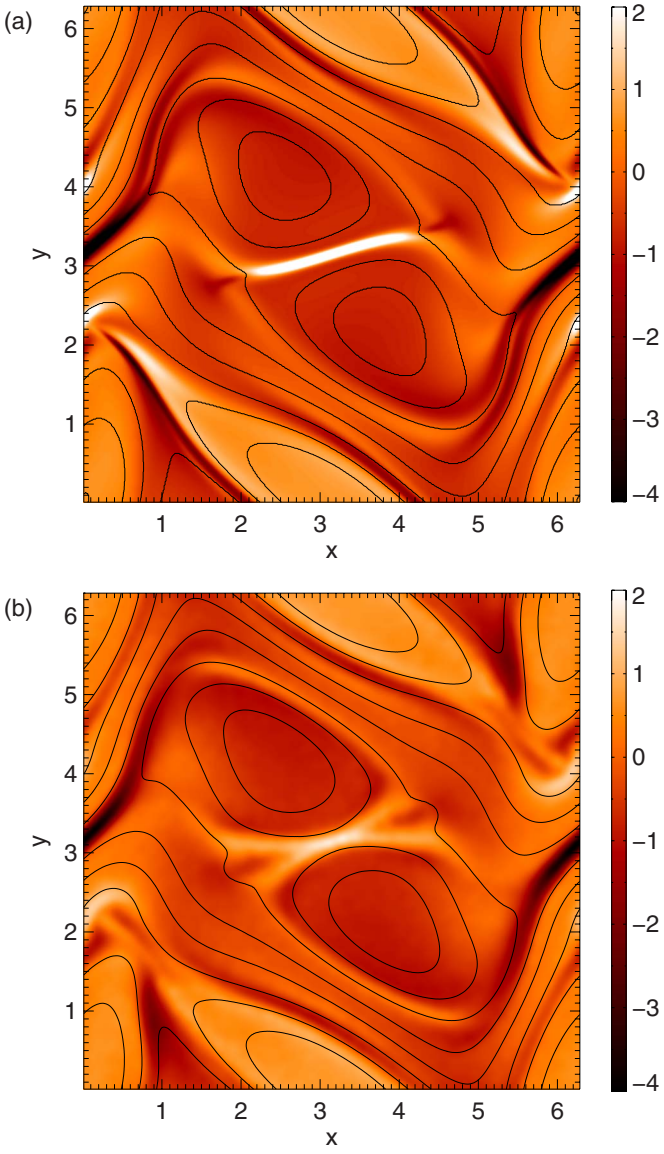

FIG. 1. (Color online) Current density with magnetic flux contours at $t=1.96$ in (a) fluid and (b) hybrid simulations.

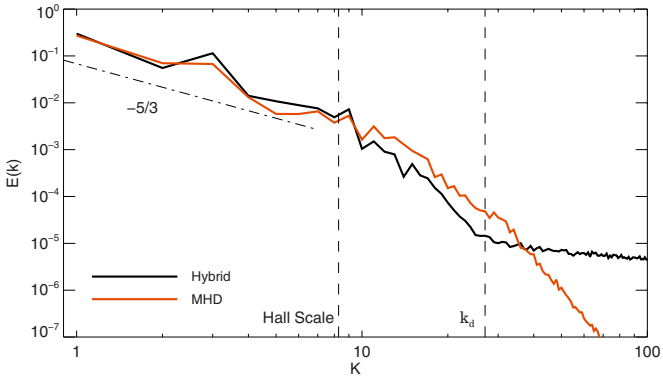

FIG. 2. (Color online) Magnetic field power spectra at $t=5.69$ for the hybrid and MHD simulations. The Hall scale and MHD Kolmorogorov dissipation scale (k_d) are shown for reference. The Hall scale, where dispersive kinetic Alfvén waves arise, occurs when $kd_i c_s/c_m \geq 1$, where c_s is the sound speed and c_m is the magnetosonic speed (Ref. 28).

While the present model is idealized and not intended to be interpreted as a representation of the solar wind, the parameter regime and geometry are roughly compatible with solar wind conditions. For example, the solar wind is usually viewed as a $\beta \sim 1$ plasma, and solar wind fluctuations are frequently characterized as quasi-two-dimensional (quasi-2D).[39] Furthermore solar wind turbulence is typically viewed as driven by large scale fluctuations or velocity shears that predominantly occur at scales much larger than the ion inertial scale.[5] Each of these characteristics is represented in a very approximate way in the present simulation model.

III. RESULTS AND DISCUSSION

The hybrid simulation results are compared to those of a compressible 2.5D MHD version of the code F3D (Ref. 40) with constant and uniform resistivity $\eta=0.0048$, zero viscosity ν, and ratio of specific heats $\gamma=5/3$. (We motivate values for η and ν later.) In both cases, the magnetic islands initially centered on the midplane ($y=\pi$) begin a clockwise rotation. The initial velocity profile shears the magnetic islands until $t\sim 2$ as the islands approach and undergo a brief period of magnetic reconnection for $t\sim 2-4$. After $t\sim 4$, the system is dominated by strong turbulence. A comparison of out-of-plane current density J_z and magnetic field lines at $t=1.96$ is shown in Fig. 1. The hybrid and MHD results show strong similarities at large scales, but significant differences at small scales where kinetic effects become important.

In the magnetic field power spectra at $t=5.69$, shown in Fig. 2, the MHD and hybrid spectra are nearly identical at small k, showing a power-law roughly consistent with a Kolmogorov $(-5/3)$, shown for reference. The two spectra diverge when the Hall scale is reached (denoted by a vertical dashed line), i.e., when the Alfvén wave becomes dispersive due to the Hall term in Ohm's law[28] at $k^2 d_i^2 (c_s^2/c_m^2) \approx 1$, where d_i is the ion inertial length, $c_s^2 = T_i/m_i$ is the sound speed, and $c_m^2 = c_s^2 + c_A^2$ is the magnetosonic speed. This effective gyroradius scale corresponds to $k \approx 8.3$. That the linear theory of Alfvén waves should so accurately predict the spectral break is surprising because the interactions are decidedly nonlinear. It should be noted that this Hall scale does not correspond to $kd_i \approx 1$, which is typically used for the scale at which parallel propagating whistlers occur. A higher k is required for the dispersive kinetic Alfvén wave to become active because the electron velocities for this wave are slower than those for a whistler at the same k. The oblique whistler is part of the high frequency magnetosonic branch and arises when $k_\parallel d_i c_A/c_m \geq 1$.[28] However, for the simulations in this study, $d_i c_A/c_m < d_e$, so electron inertia effects become important before whistlers become active, meaning that there are no oblique whistlers in this study.

It is instructive to examine the energy and dissipation budgets for the MHD and hybrid simulations, where flow energy $E_v = \langle \rho |\mathbf{v}^2|/2 \rangle$, magnetic energy $E_B = \langle |\mathbf{B}|^2/2 \rangle$, thermal energy E_{th} (total proton kinetic energy minus flow energy), and total energy E_{tot}. For the duration of this paper, $\langle \cdots \rangle$ represents a spatial average over the entire simulation domain. Grid scale fluctuations in the hybrid data are smoothed using a standard local, weighted iterative averaging.

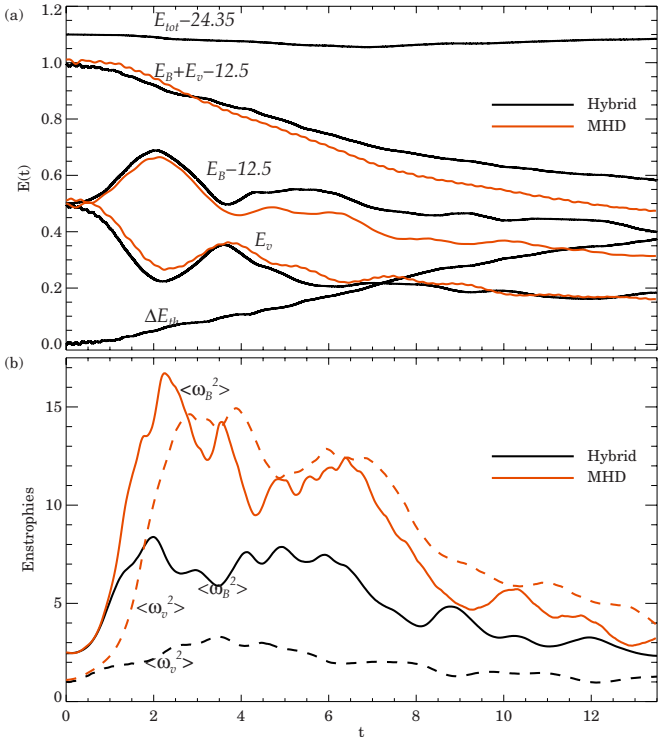

FIG. 3. (Color online) Hybrid and MHD comparison: (a) magnetic energy E_B, fluid flow energy E_v, their sum, the change in thermal energy $\Delta E_{\rm th}$, and total energy $E_{\rm tot}$ vs time. (b) Flow enstrophy $\langle\omega_v^2\rangle$ and magnetic enstrophy $\langle\omega_B^2\rangle$ vs time.

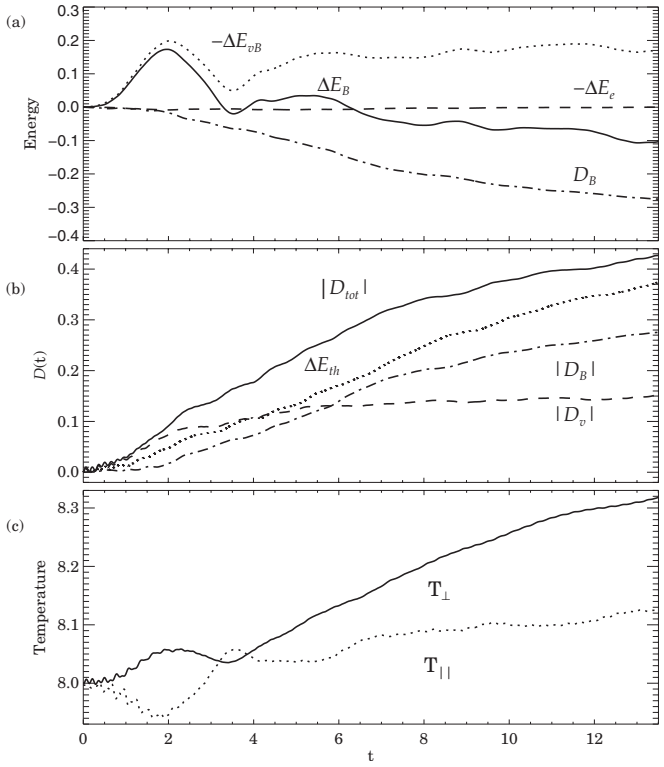

FIG. 4. (a) ΔE_B: change in E_B in the hybrid run; ΔE_{vB}: exchange between E_v and E_B; ΔE_e: electron kinetic energy; $\mathcal{D}_B$: sum of these, total E_B dissipated. (b) $\mathcal{D}_v$ and $\mathcal{D}_B$ are cumulative dissipation through bulk flow and magnetic channels, $\mathcal{D}_{\rm tot}$ their sum, $\Delta E_{\rm th}$ change in thermal energy. (c) Parallel and perpendicular proton temperatures vs time.

Figure 3(a) shows E_v, E_B, their sum, $\Delta E_{\rm th}$ (where Δ means the change since $t=0$) and $E_{\rm tot}$, as a function of time from the hybrid and MHD simulations, with E_B and $E_{\rm tot}$ shifted down by a constant for convenience. Note that $E_{\rm tot}$ changes very little over the course of the hybrid run, demonstrating good numerical energy conservation. During the initial phase ($t<2$), bulk flow energy is converted strongly into magnetic energy as field lines are stretched, but with little proton heating. The magnetic energy converts back to flow energy (with some heating) during the reconnection event ($t\sim 2$–4). Until $t\sim 4$, the energetics of the hybrid and MHD results are very similar. However, in the turbulent phase ($t>4$), the hybrid and MHD codes show significant differences, and more dissipation occurs in the MHD case. Notably, the proton thermal energy increases monotonically during the turbulent phase in the hybrid simulation.

In MHD, mean square gradients of **v** and **B** are proportional to the energy dissipation rate. Although the hybrid code lacks explicit dissipation coefficients in the ion momentum or magnetic induction equations, it is instructive to compare in Fig. 3(b) the out-of-plane enstrophy (mean square vorticity) $\langle\omega_v^2\rangle=\langle|\hat{\mathbf{z}}\cdot(\nabla\times\mathbf{v})|^2\rangle$ and out-of-plane magnetic enstrophy (mean square current density) $\langle\omega_B^2\rangle=\langle|\hat{\mathbf{z}}\cdot(\nabla\times\mathbf{B})|^2\rangle=\langle J_z^2\rangle$ in the hybrid and MHD simulations. At early time ($t<4$), the hybrid and MHD enstrophies peak at about same time, but their magnitudes are very different, indicating that the length scales in the hybrid case are larger probably due to finite Larmor radius effects. During the turbulent phase ($t>4$), the enstrophies continue to be different but the magnetic enstrophies are surprisingly similar. This suggests that the kinetic dissipation may have some resemblance to a classical resistivity, which we revisit later. Note that the value of enstrophy in the hybrid case is necessarily sensitive to the averaging that defines the fluid scales.

In order to understand the nature of the collisionless dissipation occurring during the hybrid simulations, consider the flow of magnetic energy in the system. Dotting the induction equation [Eq. (5)] with **B**, averaging over space, and integrating over time gives

$$\Delta E_B(t) = -\int_0^t \langle \mathbf{v}\cdot(\mathbf{J}\times\mathbf{B})\rangle dt' - \frac{d_e^2}{2}\langle \Delta J^2(t)\rangle - \mathcal{D}_B(t), \quad (8)$$

where any "Δ" refers to the change since $t=0$. The $\mathbf{v}\cdot(\mathbf{J}\times\mathbf{B})$ term, which will be denoted as ΔE_{vB}, is the exchange in energy between bulk flow and the magnetic field, and the d_e^2 term is essentially the electron kinetic energy. Because the total energy conservation is very good in the hybrid simulations, the first three terms in Eq. (8) can be combined to yield the cumulative energy change in the magnetic channel, denoted as $\mathcal{D}_B(t)$. Included in $\mathcal{D}_B(t)$ are kinetic dissipative processes and grid scale diffusion. Because the first three terms in Eq. (8) can be calculated directly from the simulations, it is possible to determine $\mathcal{D}_B(t)$.

For $t<4$, the energy terms in Eq. (8) are characterized by a reversible transfer of energy back and forth between the magnetic field and ion flow, as seen in Fig. 4. The magnetic energy E_B first rises and then falls, and this change is closely matched by the ion flow/magnetic energy conversion term

$-\Delta E_{vB}$. This reversible oscillation is an Alfvén wavelike response of the system as magnetic islands are stretched and then release their tension. Starting around $t\sim 4$ when the system becomes turbulent, substantial magnetic dissipation occurs (D_B decreases). The magnetic energy which is dissipated comes both directly from E_B and from flow energy which is converted to magnetic energy [E_B decreases and $(-\Delta E_{vB})$ increases]. Of the dissipated magnetic energy D_B, about half comes directly from E_B, and the other half from the ion flow/magnetic energy conversion.

A similar analysis is performed for energy flow in the bulk flow channel. Dotting the MHD momentum equation with **v** and integrating over time and space gives

$$\Delta E_v(t) = \int_0^t \langle \mathbf{v}\cdot(\mathbf{J}\times\mathbf{B})\rangle dt' - \mathcal{D}_v(t), \tag{9}$$

where $\mathcal{D}_v$ is the cumulative energy converted into heat from the flow channel through nonfluid effects and compression. Figure 4(b) shows D_v (dashed line), $\mathcal{D}_B$ (dot-dashed line), $\mathcal{D}_{\rm tot}=\mathcal{D}_B+\mathcal{D}_v$ (solid line), and $\Delta E_{\rm th}$ (dotted line). In the turbulent phase ($t>4$), there is very little energy dissipated through the flow channel ($\mathcal{D}_v$ is relatively constant). Nearly all of the change in $D_{\rm tot}$ for $t>4$ occurs due to D_B, so the main source of dissipation in this system is through magnetic interactions. The small departure between $D_{\rm tot}$ and $\Delta E_{\rm th}$ remains relatively constant during the turbulent phase and can be accounted for by the change in the total energy $E_{\rm tot}$ [see Fig. 3(a)]; this is only about 10% of the total dissipated energy. We wish to emphasize that the total energy is not an explicit constant in our equations of motion. Grid scale diffusion of magnetic energy would lead to a decrease in the total energy. Therefore, the total energy is only conserved when grid scale diffusion and other numerical effects are kept at a minimum.

Upon reflection of some basic physical arguments, it seems reasonable on physical grounds that little dissipation occurs through the flow channel. In the MHD regime (low wavenumber k), the dynamics of the hybrid simulation are at most weakly compressible, so the majority of energy is in oblique Alfvén waves that are weakly damped.[41] As energy cascades to smaller scales, from Fig. 2 it is clear that the hybrid simulation reaches the Hall scale (effective proton gyroradius shown in Fig. 2) and diverges from the MHD spectra before the MHD system reaches the Kolmogorov dissipation scale (k_d in Fig. 2). Thus, there is little dissipation in the hybrid simulation in the MHD scales where the proton flows are significant. Below the effective proton gyroradius, the ions decouple from the magnetic field and only weakly participate with the non-MHD waves in this region. Consequently, we would expect the Alfvén ratio E_v/E_B to go to zero in the kinetic regime as evidenced by the structure of kinetic Alfvén waves.

A central result of this study is that the dissipated magnetic energy preferentially heats the protons perpendicular to the mean magnetic field, as shown in Fig. 4(c). The perpendicular and parallel temperatures $T_\perp$ and $T_\parallel$ are calculated relative to the mean field (guide field). In the turbulent phase ($t>4$), $T_\perp$ increases monotonically, while $T_\parallel$ remains relatively steady. The relative anisotropy is small because the available magnetic free energy in the system (from B_x and B_y) is small compared to the proton temperature, i.e., $\beta_\perp \gg 1$. Preliminary simulations with the proton temperature reduced to 1.5 ($\beta_\perp\sim 3$) have been performed, and initial results indicate a sizable temperature anisotropy ($T_\perp/T_\parallel-1$) of around 0.303, as opposed to 0.0494 in the current study. The perpendicular heating occurs without any obvious connection to classical cyclotron resonances, as the latter generally is construed[8] to involve gyroresonance with waves propagating parallel to a background field (along the invariant direction in this study). Resonance can also involve wave frequencies near the cyclotron frequency; however, dominance in this simulation of incompressible modes and relatively low frequency kinetic Alfvén waves makes the connection to standard cyclotron resonance[8] uncertain.

We note that the perpendicular heating seen in this study is evidence that the first adiabatic invariant, $\mu=(m_i v_\perp^2)/\omega_c$, is not conserved in our simulation for at least some of the protons. As a preliminary test to be followed up in a later paper, we have stepped test particles through the static fields of the hybrid simulation and verified that often μ is not conserved when particles cross the simulation current sheets. To justify the use of static fields, we have verified that there is not significant power in the magnetic field at the cyclotron frequency. The in-plane electric fields and magnetic fields change sign across the current sheets. For simplicity, we consider only the changing magnetic fields. In order for μ to be conserved, the following parameter must be small:[42]

$$\epsilon = \frac{1}{\omega_c}\left|\frac{\partial B/\partial t}{B}\right| \sim \frac{\tau_c}{\tau}\frac{\delta B}{B}, \tag{10}$$

where τ_c is the cyclotron time and τ is the time over which the particle feels a change in δB. For reconnecting current sheets with a guide field with small electron temperature, the current sheet width is comparable to the proton Larmor radius based on the thermal speed.[28,43] Therefore $\tau_c/\tau\sim 1$ and $\delta B/B\approx 2/5$, giving $\epsilon=0.4$. There are a considerable number of protons with speeds greater than the thermal speed, which will have larger τ_c/τ and thus larger ϵ. As the guide field becomes larger, ϵ will decrease. However, to maintain μ conservation for the large majority of particles it would be necessary to have an extremely large guide field in our hybrid simulations.

The energy analysis described in this paper is summarized in Fig. 5, where the primary energy exchange is denoted with bold arrows and the dashed arrows denote very small or no energy exchange. In short, energy that was initially in bulk flows and magnetic fields is converted into proton heating during the turbulent phase. The magnetic energy dissipates directly, while the bulk flow energy is first converted into magnetic energy and then dissipated.

If we assume that the classical functional forms for the dissipation rates $\eta\langle J_z^2\rangle$ and $\nu\langle\omega_v^2\rangle$ are valid, we can compute effective transport coefficients $\eta_{\rm eff}$ and $\nu_{\rm eff}$ from the hybrid simulations. Figure 6 shows $\eta_{\rm eff}=(\partial\mathcal{D}_B/\partial t)/\langle J_z^2\rangle$ and $\nu_{\rm eff}=(\partial\mathcal{D}_v/\partial t)/\langle\omega_v^2\rangle$ versus time. Surprisingly, the spatially averaged $\eta_{\rm eff}$ is fairly constant in time, as is often assumed in

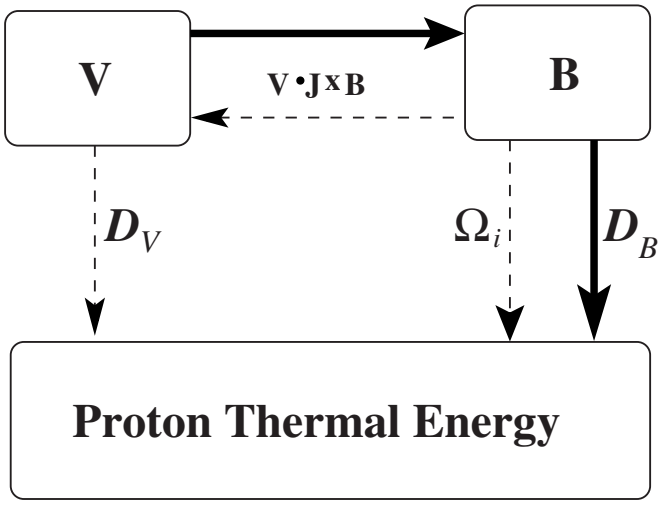

FIG. 5. Flow of energy through the turbulent hybrid simulations. Bold arrows denote significant energy conversion through a channel. Light dashed arrows denote little or no energy conversion through a channel. Ω_i represents cyclotron damping, D_B represents magnetic dissipation, and D_v represents dissipation of proton bulk flow.

MHD models. The mean value is $\eta_{\text{eff}}=0.0043$, corresponding to a magnetic Reynolds number of $S_{\text{eff}}=L/\eta_{\text{eff}}\approx 1461$, which motivated the value used in the MHD simulation. In classical turbulence theory, the length scale at which dissipation occurs λ_d is related to the Reynolds number and energy containing scale L through $S_{\text{eff}}\sim(L/\lambda_d)^{4/3}$.[44] For the hybrid simulation, $\lambda_d\sim 0.0266$, which is in the order of the electron skin depth, $c/\omega_{pe}\sim 0.049$. The spatially averaged ν_{eff}, on the other hand, shows oscillations much larger than the mean, calling into question the assumption of a nonzero viscosity assumed in many MHD models.

The effective resistivity being fairly constant does not imply that the dissipation is in the form ηJ^2. The MHD simulations performed with this η_{eff} show more dissipation of B than the hybrid simulations and cannot reproduce the preferential heating of $T_\perp$.

This study presents one of the first self-consistent simulations to show anisotropic heating of protons and is an important first step to understanding collisionless dissipation in turbulence on the sun and in the solar wind. There are limitations to the scope of this study, however. Primarily, the simulations in this study are 2D, with no variation allowed along the direction of the mean magnetic field. As such, Landau damping and transit-time damping due to particle motion along this mean magnetic field are not present. It is possible, therefore, that parallel heating from these two effects could boost the parallel proton temperature and minimize or even reverse the anisotropy seen in these simulations. Three-dimensional hybrid simulations are planned for future studies which will address this issue. Future studies will also investigate the spatial dependence of η_{eff} and its dependence on electron/proton inertial lengths, as well as system size. We will also examine the effect of reducing the guide field and including electron pressure in Ohm's law. The specific microscopic physical mechanism, which converts magnetic energy into proton heat, remains an open question and is under investigation.

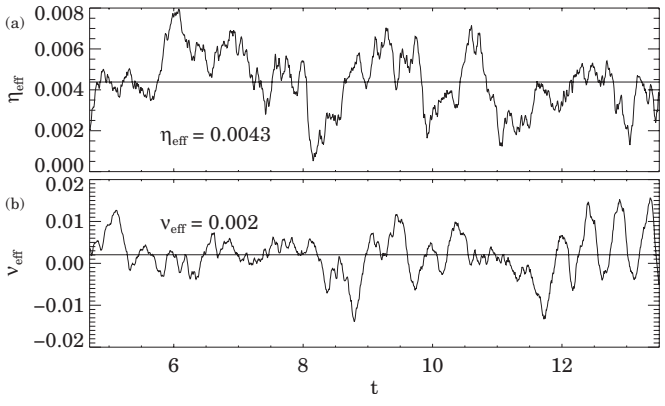

FIG. 6. Effective (a) resistivity η and (b) viscosity ν vs time.

ACKNOWLEDGMENTS

This work was supported by NSF Grant No. ATM-0539995, NSF Grant No. ATM-0645271, NASA Grant No. NNG05GM98G, NASA Grant Nos. NNX08AT76G (MMS Theory Support) and NNX-08AI47G (Heliophysics Theory program), and NERSC. The authors thank S. Servidio, S. P. Gary, and B. N. Rogers for enlightening conversations.

[1] S. Cranmer, Space Sci. Rev. **101**, 229 (2002).
[2] C. Smith, K. Hamilton, B. Vasquez, and R. Leamon, Astrophys. J. Lett. **645**, L85 (2006).
[3] D. Sundkvist, A. Retinò, A. Vaivads, and S. D. Bale, Phys. Rev. Lett. **99**, 025004 (2007).
[4] S. Spangler, Astron. Astrophys. **407**, 563 (2003).
[5] C. Tu and E. Marsch, Space Sci. Rev. **73**, 1 (1995).
[6] J. McKenzie, M. Banaszkiewicz, and W. Axford, Astron. Astrophys. **303**, L45 (1995).
[7] C. Tu and E. Marsch, Sol. Phys. **171**, 363 (1997).
[8] P. Isenberg, M. Lee, and J. Hollweg, J. Geophys. Res. **106**, 5649, DOI: 10.1029/2000JA000099 (2001).
[9] D. Montgomery and L. Turner, Phys. Fluids **24**, 825 (1981).
[10] J. Shebalin, W. Matthaeus, and D. Montgomery, J. Plasma Phys. **29**, 525 (1983).
[11] G. Zank and W. Matthaeus, Phys. Fluids A **5**, 257 (1993).
[12] C. S. Ng and A. Bhattacharjee, Astrophys. J. **465**, 845 (1996).
[13] B. Chandran, Phys. Rev. Lett. **95**, 265004 (2005).
[14] B. D. G. Chandran, Phys. Rev. Lett. **101**, 235004 (2008).
[15] W. Matthaeus, D. Mullan, P. Dmitruk, L. Milano, and S. Oughton, Nonlinear Processes Geophys. **10**, 93 (2003).
[16] P. Dmitruk, W. H. Matthaeus, and N. Seenu, Astrophys. J. **617**, 667 (2004).
[17] S. R. Cranmer and A. A. van Ballegooijen, Astrophys. J. **594**, 573 (2003).
[18] S. A. Markovskii, B. J. Vasquez, C. W. Smith, and J. V. Hollweg, Astrophys. J. **639**, 1177 (2006).
[19] S. Ghosh, E. Siregar, D. A. Roberts, and M. L. Goldstein, J. Geophys. Res. **101**, 2493, DOI: 10.1029/95JA03201 (1996).
[20] P. Dmitruk and W. Matthaeus, Phys. Plasmas **13**, 042307 (2006).
[21] M. L. Goldstein, S. Ghosh, E. Sireger, and V. Jayanthi, Lect. Notes Phys. **536**, 269 (1999).
[22] P. S. Gary, L. Yin, and D. Winske, J. Geophys. Res., [Space Phys.] **111**, A06105, DOI: 10.1029/2005JA011552 (2006).
[23] F. Valentini, P. Veltri, F. Califano, and A. Mangeney, Phys. Rev. Lett. **101**, 025006 (2008).
[24] K. Bowers and H. Li, Phys. Rev. Lett. **98**, 035002 (2007).
[25] G. Howes, W. Dorland, S. Cowley, G. Hammett, E. Quataert, A. Schekochihin, and T. Tatsuno, Phys. Rev. Lett. **100**, 065004 (2008).
[26] P. S. Gary, S. Saito, and H. Li, Geophys. Res. Lett. **35**, L02104, DOI: 10.1029/2007GL032327 (2008).
[27] S. Orszag and C. Tang, J. Fluid Mech. **90**, 129 (1979).

[28]B. Rogers, R. Denton, J. Drake, and M. Shay, Phys. Rev. Lett. **87**, 195004 (2001).
[29]R. Dahlburg and J. Picone, Phys. Fluids B **1**, 2153 (1989).
[30]D. Rosenberg, A. Pouquet, and P. D. Mininni, New J. Phys. **9**, 304 (2007).
[31]A. Matthews, R. Grappin, A. Mangeney, and J. Léorat, Lect. Notes Phys. **462**, 399 (1995).
[32]J. Birn, J. F. Drake, M. A. Shay, B. N. Rogers, R. E. Denton, M. Hesse, M. Kuznetsova, Z. W. Ma, A. Bhattacharjee, A. Otto, and P. L. Pritchett, J. Geophys. Res., [Space Phys.] **106**, 3715, DOI: 10.1029/1999JA900449 (2001).
[33]M. A. Shay, J. F. Drake, R. E. Denton, and D. Biskamp, J. Geophys. Res., [Space Phys.] **103**, 9165, DOI: 10.1029/97JA03528 (1998).
[34]M. A. Shay, J. F. Drake, B. N. Rogers, and R. E. Denton, Geophys. Res. Lett. **26**, 2163, DOI: 10.1029/1999GL900481 (1999).
[35]M. A. Shay, J. F. Drake, B. N. Rogers, and R. E. Denton, J. Geophys. Res., [Space Phys.] **106**, 3759, DOI: 10.1029/1999JA001007 (2001).
[36]K. Malakit, P. A. Cassak, M. A. Shay, and J. F. Drake, "The Hall effect in magnetic reconnection: Hybrid vs. Hall-less hybrid simulations," Geophys. Res. Lett. (in press).
[37]C. K. Birdsall and A. B. Langdon, *Plasma Physics via Computer Simulation* (McGraw-Hill, New York, 1985), pp. 20–22.
[38]G. G. Howes, S. C. Cowley, W. Dorland, G. W. Hammett, E. Quataert, and A. A. Schekochihin, Astrophys. J. **651**, 590 (2006).
[39]J. Bieber, W. Wanner, and W. Matthaeus, J. Geophys. Res. **101**, 2511, DOI: 10.1029/95JA02588 (1996).
[40]M. Shay, J. Drake, M. Swisdak, and B. Rogers, Phys. Plasmas **11**, 2199 (2004).
[41]S. Gary, J. Geophys. Res. **104**, 6759 DOI: 10.1029/1998JA900161 (1999).
[42]N. A. Krall and A. W. Trivelpiece, *Principles of Plasma Physics* (McGraw-Hill, New York, 1973).
[43]R. Kleva, J. Drake, and F. Waelbroeck, Phys. Plasmas **2**, 23 (1995).
[44]G. K. Batchelor, *The Theory of Homogeneous Turbulence* (Cambridge University Press, New York, 1953).